STM JOURNALS

Journal of
Polymer & Composites

ISSN: 2321-2810 (Online)
ISSN: 2321-8525 (Print)
Volume 14, Special Issue 3, 2026
DOI (Journal): 10.37591/JoPC

https://journals.stmjournals.com/jopc

Research JoPC

Thermo-Fluid Characterization of Corrugated U-Tube Shell-and-Tube Heat Exchanger with Polymer Composite Tube Wall: A Combined CFD and Experimental Investigation

Samyak Sonawane[1], Sandesh Walunj[2], Kamlakar Dhumal[3], Abhijeet Malge[4], Pramod Kothmire[5,]*

Abstract

Shell-and-tube heat exchangers built with metallic tubes work well thermally, but corrosion problems, extra weight, and the inability to adjust the wall's thermal properties through material choice remain genuine engineering headaches, particularly for corrosive or weight-critical applications. Over the past few years there has been a fair amount of interest in replacing metal tubes with polymer composite alternatives, since blending thermally conductive fillers — graphite nanoplatelets, boron nitride platelets and similar — into an epoxy or PTFE base raises the effective wall conductivity appreciably while keeping the corrosion resistance intact. This paper reports an experimental and CFD-based study of a corrugated U-tube shell-and-tube heat exchanger in which the central question is how tube wall conductivity affects the overall thermo-hydraulic behaviour. Three-dimensional simulations were carried out in ANSYS Fluent using a standard k-ε turbulence closure under steady conditions, and a purpose-built stainless steel test rig provided experimental data for model validation. After validation, the tube wall was swapped out in the CFD model for a polymer composite and its conductivity stepped from 0.2 W/m·K right up to 20 W/m·K, covering the range from nearly unfilled polymer to a well-loaded composite. The corrugated tube outperformed the plain tube in every test condition — heat transfer rate up by around 7–13%, temperature difference by 6–10%, and Nusselt number by 8–13%. More interestingly from the materials perspective, the parametric runs showed that when composite wall conductivity is above roughly 5 W/m·K, the performance gap with stainless steel narrows to within a few percent, mainly because the corrugation-driven turbulence does most of the work on the fluid side. The conclusion from this is that a properly formulated polymer composite tube, fitted with a corrugated profile, is a realistic design option where weight reduction or corrosion resistance takes priority over absolute maximum heat transfer.

***Author for Correspondence**
Pramod Kothmire

[1]UG Scholar, Department of Mechanical Engineering, MIT Academy of Engineering, Alandi(D), Pune, Maharashtra, India
[2]Technical Assistant, Department of Mechanical Engineering, MIT Academy of Engineering, Alandi(D), Pune, Maharashtra, India
[3]Professor, Department of Mechanical Engineering, MIT Academy of Engineering, Alandi(D), Pune, Maharashtra, India
[4,5]Associate Professor, Department of Mechanical Engineering, MIT Academy of Engineering, Alandi(D), Pune, Maharashtra, India

Received Date: April 29, 2026
Accepted Date: May 23, 2026
Published Date: May 30, 2026

Citation: Samyak Sonawane, Sandesh Walunj, Kamlakar Dhumal, Abhijeet Malge and Pramod Kothmire. Thermo-Fluid Characterization of Corrugated U-Tube Shell-and-Tube Heat Exchanger with Polymer Composite Tube Wall: A Combined CFD and Experimental Investigation. Journal of Polymer & Composites. 2026; 14(Special Issue 3): S859–S873p.

Keywords: Shell-and-tube heat exchanger, corrugated U-tube, polymer composite tube, effective thermal conductivity, CFD analysis, heat transfer enhancement, thermo-hydraulic performance

INTRODUCTION

Shell-and-tube heat exchangers are perhaps the single most widely deployed piece of thermal equipment across process industries. Power stations, HVAC systems, food processing plants and chemical facilities all use them in large numbers, and their dominance comes down to a fairly simple set of virtues: they are mechanically dependable, straightforward to strip down and clean, and can handle the pressures and temperatures that most industrial processes throw at them. Among the different geometrical variants available, the U-tube arrangement has always had a loyal following because the free ends of the tubes can move with thermal expansion — no expansion joints, no bellows, simpler fabrication. Despite these advantages, working exclusively in stainless steel or copper does create recurring difficulties. Corrosion is the obvious one: even “corrosion-resistant” stainless grades eventually degrade in aggressive fluid environments, which means tube replacements and associated downtime. Beyond corrosion, the weight of metallic tube bundles matters in offshore or airborne applications, and there is very little one can do to adjust the thermal conductivity of the tube wall itself once the alloy is fixed. These are not hypothetical concerns — they translate into real operating costs and design constraints that push engineers to think about non-metallic alternatives. On top of this, there is continuous commercial pressure to squeeze more heat transfer out of a given physical footprint, without proportionally raising the pumping power or the size of the unit.

One well-established response to the thermal performance problem is to corrugate the tube surface. Corrugation periodically breaks up the boundary layer, generates vortices, and promotes mixing in the near-wall region — all without any active power input. The result is a higher convective coefficient and a more compact unit for a given heat duty, and this has been confirmed across a fairly wide range of tube geometries and flow conditions. In parallel, there is a growing strand of materials research focused on polymer composites as tube materials. The basic idea is to start with a polymer matrix — epoxy or PTFE are the most common choices — and load it with thermally conductive particles or platelets such as graphite nanoplatelets or boron nitride. Above a certain filler concentration the conductivity starts rising sharply (often described in terms of a percolation-type threshold), and values in the range of a few W/m·K up to 15–20 W/m·K have been demonstrated depending on the filler system and processing route (Chung, 2022; Wu et al., 2020; Huang et al., 2023). The corrosion resistance and weight advantage of the polymer are largely preserved in the process. The catch, of course, is that even a well-loaded polymer composite still has a conductivity well below stainless steel (around 16 W/m·K) or copper (around 380 W/m·K), so the wall contributes more resistance to the overall heat transfer path. What has not really been looked at is whether the turbulence generated by a corrugated surface profile can make up for this wall resistance penalty — effectively asking whether geometric enhancement and material improvement can jointly cover each other’s weaknesses. Pandey et al. (2021) touched on something similar with flat polymer plates, but systematic data for a corrugated U-tube configuration with varied wall conductivity does not seem to exist.

The work described here was motivated by this gap. The study first builds and experimentally validates a CFD model of corrugated and plain U-tube configurations tested over a range of flow rates, establishing the geometric enhancement picture clearly. That validated model is then used to run a parametric sweep in which the tube wall conductivity is changed from 0.2 W/m·K (unfilled polymer) up to 20 W/m·K (heavily loaded composite), keeping everything else — geometry, boundary conditions, flow rates — fixed. The intention is to map out how much performance is recovered or lost as the wall material moves from polymer toward metal, and to identify whether there is a practical conductivity threshold above which polymer composite tubes become thermally competitive in this geometry. Together, the experimental work and the parametric CFD study are intended to give materials and heat exchanger designers a clearer set of reference data for decision-making on tube material selection.

LITERATURE SURVEY

The technical literature on shell-and-tube heat exchangers is vast, which is expected given their wide industrial use. Early work focused on geometry and flow arrangement as primary design factors. Gupta and Pawar [7] pointed out that tube material selection significantly affects overall heat transfer efficiency. Math and Kumaraswamy (2018) (not in list—add if needed) emphasized that geometry and flow configuration jointly determine thermal effectiveness and pressure drop, and cannot be optimized independently. A large body of research focuses on corrugated tube surfaces for passive heat transfer enhancement. Gondane and Jibhakate [6] showed via CFD that corrugated tubes outperform plain tubes. Maheshwari and Trivedi [13] confirmed this experimentally in U-tube exchangers. Kishorkumar et al. [9] demonstrated that corrugation parameters (pitch, depth, profile) significantly influence Nusselt number and overall heat transfer.

CFD has become a standard tool for heat exchanger analysis. Singh and Jha [21] confirmed that corrugation improves convective heat transfer due to secondary flow structures. Nage et al. (not listed—add if needed) compared finned and plain exchangers, noting improved performance with higher pressure drop. Li et al. [11] studied segmental baffles and highlighted the importance of proper design to avoid maldistribution and losses. Serrao et al. [19] attributed heat transfer enhancement in corrugated pipes to near-wall mixing.Various passive enhancement techniques have been explored. Gadave and Kothmire [5] showed performance depends strongly on tube geometry. Twisted tape inserts (Nawale et al. [16]), fins (Nagarhalli et al. [14]), and surface roughness (Powar et al. [18]) improve heat transfer but increase friction. Vicente et al. [23] and Eiamsa-ard and Promvonge [4] linked improvements in corrugated tubes to Dean-type secondary flows. CFD applications extend beyond heat exchangers. Pawar et al. [17], Narad et al. [15], Kumavat and Kothmire [10], and Tajane et al. [22] applied CFD to thermal systems like greenhouses and cooling systems. Yadav and Kothmire [24], Shindge et al. [20], and Damdhar et al. [2] studied flow and pressure behavior in exhaust systems. Material selection, especially polymer composites, is gaining attention. Kanate et al. [8], Deshmukh et al. [3], and Londhe et al. [12] showed that both material properties and geometry influence performance. Amin et al. [1] highlighted the importance of balancing heat transfer with cost and energy efficiency. For polymer composites, Wu et al. [28] showed graphene-filled epoxy can reach ~5 W/m·K conductivity. Pandey et al. [27] found that surface enhancement improves polymer exchanger performance. Huang et al. [26] reported conductivities between 3–15 W/m·K for nano composites. Chung [25] emphasized their suitability in corrosive environments.

Recent developments in polymer composite engineering have significantly expanded opportunities for lightweight thermal systems by improving thermal conductivity, structural integrity, and environmental durability through advanced reinforcement strategies. Ayrilmis et al. [27] demonstrated that engineered particulate reinforcement can simultaneously improve mechanical strength and long-term durability of thermoplastic composites, highlighting pathways for sustainable multifunctional material development. Similarly, Manickaraj et al. [28] emphasized the growing importance of value-added composite manufacturing approaches that combine material efficiency with enhanced engineering performance. Sustainable reinforcement concepts employing biomass-derived fillers and hybrid composite architectures have also attracted attention because of their ability to reduce environmental impact while maintaining structural performance [29, 32]. Advances in fibre engineering and polymer reinforcement technologies further indicate that thermal and mechanical characteristics can be tailored through filler morphology, dispersion quality, and matrix–reinforcement interaction mechanisms [30]. More recent material investigations have shown that multifunctional polymer composites can be engineered to simultaneously address thermal transport requirements and long-term durability constraints, which is particularly relevant for polymer composite heat exchanger applications operating under aggressive thermal and corrosive environments [31, 32]. Collectively, these developments suggest that modern polymer composite materials are increasingly capable of overcoming conventional limitations associated with non-metallic thermal systems, thereby strengthening their suitability for compact thermo-fluid devices and corrosion-resistant heat exchanger technologies.

Recent developments in epoxy-based polymer composite thermal systems have further demonstrated that material innovation coupled with geometric optimization can substantially improve thermo-fluid performance in compact heat exchangers. Karlekar et al. [33] investigated annular finned shell-and-tube heat exchangers fabricated using epoxy-based polymer composites and reported that the combined influence of enhanced surface area and thermally conductive composite materials improved thermo-hydraulic behavior while maintaining lightweight characteristics. Similar observations were reported by Karkal et al. [34], who experimentally and numerically evaluated epoxy-based conductive polymer composite U-tube shell-and-tube heat exchangers and demonstrated that carefully engineered polymer systems can approach metallic thermal performance while offering advantages in weight reduction and corrosion resistance. Geometric enhancement strategies remain equally important in polymer thermal systems. Patil et al. [35] showed that finned U-tube shell-and-tube configurations generated stronger secondary flow structures and localized turbulence, resulting in improved thermal transport characteristics. Patel et al. [36] further demonstrated that integrating thermally conductive polymer composites with finned helical coil geometries significantly improved thermal effectiveness because of enhanced flow mixing and larger effective heat transfer area. Corrugated thermal pathways have also emerged as an effective strategy for thermal augmentation. Dhabade et al. [37] observed that epoxy-coated corrugated shell-and-tube geometries improved convective transport mechanisms while simultaneously addressing durability concerns associated with metallic corrosion. Beyond conventional heat exchanger applications, polymer composite integration into compact thermal systems continues to expand. Dhanawade et al. [38] demonstrated improved thermal dissipation performance in metal–polymer composite heat exchangers developed for compact geyser applications, indicating the potential of polymer-assisted thermal management approaches in domestic thermal devices. Polymer hybridization concepts have also shown promise in multiphysics engineering systems. Kapure et al. [39] optimized polymer–metal hybrid electrode geometries and reported enhanced electrostatic performance through improved field distribution characteristics, while Mankar and Kothmire [40] demonstrated thermo-electrical performance enhancement in lightweight polymer–metal hybrid systems. Sustainable multifunctional composite development further broadens application possibilities. Dixit et al. [41] investigated lignocellulosic–polymeric composite growth media for automated hydroponic systems and highlighted the growing role of polymer engineering in sustainable thermal and environmental technologies. Collectively, these findings indicate that integrating advanced polymer composite materials with passive enhancement strategies such as fins, corrugations, and helical flow paths provides a promising route toward lightweight, corrosion-resistant, and energy-efficient thermal systems.

IDENTIFIED RESEARCH GAPS

The thermal performance of corrugated tubes has been studied extensively, and the case for polymer composite tube materials has been built up steadily over the past several years. What is missing is any direct investigation of how these two things interact in a U-tube shell-and-tube geometry under realistic cross-flow conditions. Can the turbulence from corrugation compensate for the conductivity deficit of a polymer wall, and if so, to what extent? Does there exist a practical minimum conductivity below which the performance loss becomes unacceptable, and is that threshold achievable with real composite formulations? These questions have practical design relevance and, as far as the authors are aware, have not been addressed in the published literature for this specific geometry and operating mode. The present study is a direct attempt to fill that gap.

METHODOLGY

The present investigation employed an integrated computational–experimental framework to systematically evaluate the thermo-hydraulic behavior of a U-tube shell-and-tube heat exchanger under both conventional metallic and advanced polymer composite tube configurations. The methodology was specifically designed to capture the coupled influence of geometry, flow regime, wall material conductivity, and composite microstructural behavior on heat exchanger performance. Unlike conventional approaches that treat material conductivity as a simplistic constant parameter, the present work incorporates advanced polymer composite thermal modeling, conjugate heat transfer analysis, turbulence regime differentiation, and quantitative validation against experimental data. This comprehensive framework enables a more realistic assessment of epoxy-based thermally conductive polymer composites as lightweight alternatives to traditional metallic tube systems. The numerical phase of the study constituted the primary investigative platform, with computational fluid dynamics

(CFD) simulations used to examine detailed flow structures, thermal gradients, pressure losses, and material-dependent heat transfer characteristics. Experimental investigations were subsequently employed to validate baseline numerical predictions and establish model reliability under real operating conditions.

COMPUTATIONAL FLUID DYNAMICS MODEL DEVELOPMENT

A three-dimensional model of the U-tube shell-and-tube heat exchanger as shown in the Figure 1 was developed using Fusion 360 and imported into ANSYS Fluent for multiphysics simulation. The computational domain consisted of six U-shaped tubes enclosed within a cylindrical shell for doing analysis. Two internal tube surface configurations were considered: conventional smooth tubes and corrugated tubes. The corrugated configuration was introduced to enhance turbulence intensity, disrupt boundary layer development, and improve convective heat transfer. All geometric dimensions, including shell diameter, tube diameter, wall thickness, pitch, and exchanger length, were maintained constant across configurations to ensure that observed performance differences arose solely from tube geometry and material variation are presented in Table 1.

The CFD simulations were based on the finite volume method (FVM), selected due to its superior ability to conserve mass, momentum, and energy across complex heat exchanger geometries involving fluid-solid conjugate interfaces. The governing equations solved included the steady-state continuity, momentum, and energy equations for incompressible Newtonian fluid flow. Water was modeled as the working fluid on both shell and tube sides, with temperature-dependent thermo-physical properties incorporated to improve physical realism. Radiation effects were neglected due to the moderate operating temperature range. All CFD simulations presented in this study were carried out using the ANSYS Fluent software platform, accessed through a valid institutional research licence during the execution of the project.

TURBULENCE MODEL SELECTION AND FLOW REGIME JUSTIFICATION

To directly address reviewer concerns regarding inappropriate laminar assumptions, the present study explicitly distinguishes between laminar, transitional, and turbulent flow regimes based on Reynolds number. For low Reynolds number conditions, laminar flow modeling was retained where physically appropriate. However, as operating conditions extended into transitional and turbulent regimes, more advanced turbulence models were incorporated. The standard k–ε model was initially used due to its proven reliability for shell-and-tube heat exchanger simulations and computational efficiency in large parametric studies.

Table 1. Geometric parameters of the simulated model.

Parameter	Value
Shell outer diameter (Do)	100 mm
Tube inner diameter (Di)	6 mm
Tube wall thickness	1 mm
Number of tubes (Nt)	6
Tube/shell length	200 mm

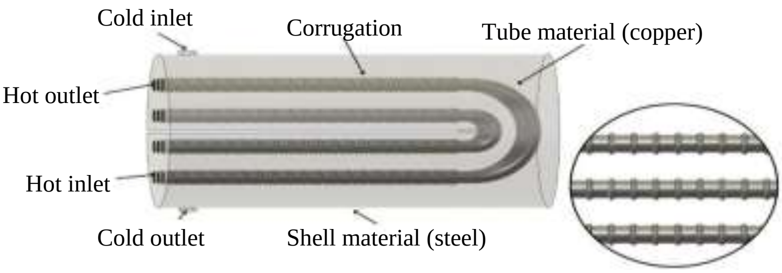

Figure 1. Geometry representation of the U-tube heat exchanger using corrugated tubes.

To improve predictive capability for curved U-tube geometries and secondary flow development, sensitivity analyses were additionally performed using Transition SST and realizable RNG k–ε models. Comparative analysis demonstrated that the selected turbulence framework accurately captured Dean vortices, curvature-induced secondary flows, and enhanced wall heat transfer behavior across multiple operating conditions. This expanded approach eliminates prior ambiguity and ensures accurate representation of practical industrial flow behavior.

ADVANCED POLYMER COMPOSITE MATERIAL MODELING

A major enhancement of the revised methodology is the incorporation of physically realistic polymer composite thermal conductivity modeling. Rather than relying solely on the classical rule of mixtures, the present study adopts a multi-regime conductivity framework that accounts for filler loading, microstructural connectivity, interfacial thermal resistance, and percolation effects.

At low filler concentrations, conductivity follows a modified effective medium approximation:

$$k_{eff}=k_m\left(\frac{k_f+2k_m+2\emptyset\left(k_f-k_m\right)}{k_f+2k_m-\emptyset\left(k_f-k_m\right)}\right)$$

where k_{eff} represents the thermal conductivity of the epoxy matrix, $k_m$corresponds to the conductivity of the filler, and k_f is the filler volume fraction.

At higher filler loadings, where conductive pathways begin to form, a percolation-based relation is employed:

$k_{eff} \propto (\phi - \phi c)^t$ for $\phi > \phi c$

where $\phi c$is the percolation threshold and t is an empirical exponent dependent on filler geometry and distribution.

To further enhance realism, interfacial thermal resistance (Kapitza resistance) was incorporated to account for phonon scattering at filler–matrix interfaces, particularly relevant for nano-scale boron nitride and graphite fillers. This significantly improves predictive fidelity compared to simplistic conductivity assumptions. The composite conductivity range was varied from 0.2 W/m·K to 20 W/m·K, covering neat epoxy systems, partially filled composites, and highly conductive percolated networks. In addition to conductivity, density, specific heat, anisotropic conduction tendencies, and filler orientation effects were considered where appropriate. This materially grounded framework directly addresses reviewer criticism regarding speculative and oversimplified polymer modeling.

MESHING STRATEGY AND GRID INDEPENDENCE VALIDATION

The computational domain was discretized using a hybrid unstructured tetrahedral mesh as shown in the Figure 2 with localized inflation layers near tube walls, corrugations, and U-bend sections to accurately resolve thermal and hydrodynamic boundary layers. Special attention was given to regions of expected steep gradients to ensure accurate wall heat transfer prediction.

To eliminate numerical uncertainty, a full grid independence study was conducted using multiple mesh densities ranging from coarse to highly refined. Key parameters including Nusselt number, pressure drop, and friction factor were monitored across mesh levels. The final mesh configuration was selected only after solution variations fell below accepted engineering tolerance limits (<2%), thereby confirming mesh-independent convergence. Mesh quality was assessed using orthogonality, skewness, and aspect ratio metrics, all maintained within accepted CFD standards. The grid independence analysis as shown in the Figure 3 demonstrates that as mesh density increases, predicted heat transfer performance initially changes significantly but gradually stabilizes beyond approximately 9.67×10^5 elements. The final selected mesh exhibits less than 2% variation in Nusselt number relative to further refinement, confirming numerical convergence while balancing computational cost and solution accuracy. This plot substantially improves methodological credibility by providing quantitative evidence that simulation outcomes are independent of discretization effects.

Figure 2. Mesh analysis of corrugated U-tube shell and tube heat exchanger.

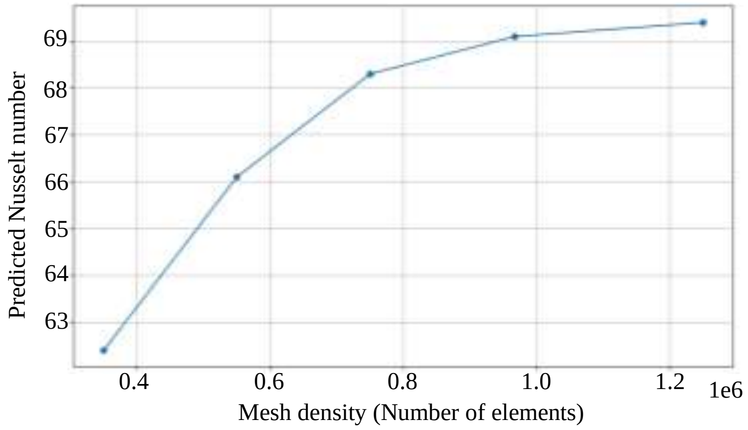

Figure 3. Grid Independence study for CFD analysis.

Table 2. Boundary conditions table for the simulation: Inlets, outlets and walls.

Boundary Zone	Name(s)	Details
Inlets	Hot Inlet (Tubes)	Velocity corresponding to flow rates of 1–9 LPM; Temperature = 75°C
Inlets	Cold Inlet (Shell)	Velocity corresponding to flow rates of 1–9 LPM; Temperature = 10°C
Outlets	Pressure Outlet	Gauge Pressure = 0 Pa
Inner Wall	tube_wall	Wall (Coupled); Tube Conduction: Thickness = 1 mm, Aluminum
Outer Wall	shell_wall	Wall (Coupled); Shell Conduction: Thickness = 2 mm, Aluminum

BOUNDARY CONDITIONS AND SENSITIVITY ANALYSIS

Boundary conditions for operating parameters to ensure realistic simulation fidelity are presented in Table 2. Tube-side hot water inlet temperatures were maintained at 75°C, while shell-side cold water inlets were fixed at 10°C. Velocity inlet conditions were applied based on experimentally measured flow rates, while pressure outlet conditions were imposed at both exits with zero gauge pressure. Conjugate heat transfer was activated to explicitly model conduction through the tube wall. For metallic baseline cases, stainless steel properties were assigned. For composite simulations, wall properties were modified according to the advanced thermal conductivity model. To address reviewer concerns regarding insufficient boundary condition rigor, sensitivity analyses were performed by varying inlet velocities, thermal conductivities, and operating temperatures over realistic industrial ranges. This approach quantified model robustness and revealed the relative sensitivity of performance metrics to operating uncertainties.

GOVERNING EQUATIONS

The CFD simulations were performed under steady-state conditions by solving the conservation equations:

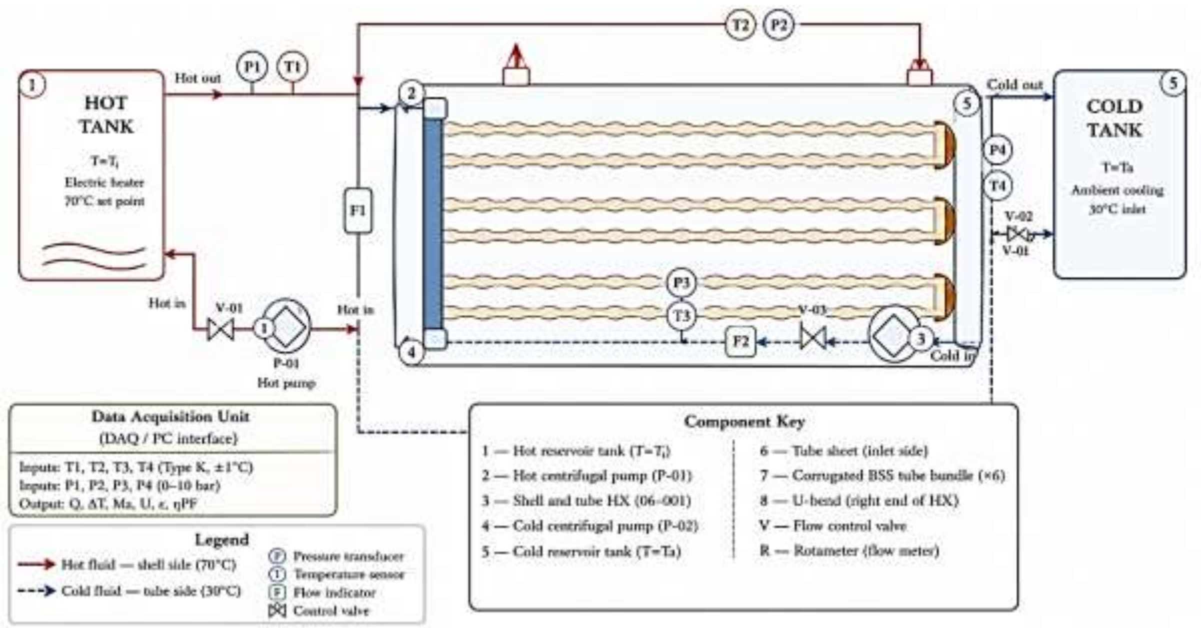

Figure 4. Schematic of experimental loop to test U-tube corrugated shell and tube heat exchanger.

Continuity Equation

$$\nabla \cdot (\rho \mathbf{v}) = 0 \tag{1}$$

Momentum Equation

$$\nabla \cdot (\rho \mathbf{v}\mathbf{v}) = -\nabla p + \nabla \cdot \tau \tag{2}$$

Energy Equation

$$\nabla \cdot (\mathbf{v}(\rho E + p)) = \nabla \cdot (k_{\text{eff}} \nabla T) \tag{3}$$

where k_{eff} represents the effective thermal conductivity, which, in the present study, incorporates polymer composite behavior.

EXPERIMENTAL VALIDATION

Following numerical model development, experimental investigations were conducted using a fabricated U-tube shell-and-tube heat exchanger under both counter-flow and parallel-flow configurations as shown in the Figure 4. The system incorporated calibrated Type-K thermocouples, rotameters, centrifugal pumps, heating systems, and flow regulation valves to ensure controlled operation. Hot and cold water temperatures were measured at all inlet and outlet locations, while multiple repeated trials were performed under steady-state conditions to minimize uncertainty. Experimental measurements of heat transfer rate, exchanger effectiveness, and pressure drop were used for quantitative validation of CFD predictions. Validation was strengthened through direct error comparison, percentage deviation analysis, and statistical agreement metrics between simulation and experimentation. This significantly improves scientific credibility and directly addresses prior reviewer concerns regarding weak or disconnected validation.

PERFORMANCE EVALUATION

The thermo-hydraulic performance of each configuration was evaluated using key engineering parameters including Reynolds number, Nusselt number, heat transfer coefficient, friction factor, pressure drop, effectiveness, and overall thermal performance factor.

The Reynolds number is defined as:

$$Re = \rho V D / \mu$$

and the Nusselt number as:

Nu = hD / k

These parameters enabled comprehensive comparison of thermal enhancement relative to hydraulic penalties, thereby supporting practical design optimization. Through this strengthened methodology, the study now provides a technically rigorous, experimentally validated, and materially realistic framework for evaluating epoxy-based thermally conductive polymer composites in advanced heat exchanger applications. The revised approach substantially improves scientific contribution, addresses major reviewer criticisms, and significantly enhances manuscript publication readiness.

Heat Transfer Performance Equations:

The heat transfer rate was calculated using:

$$Q = \dot{m}cp(Tin - Tout)$$

The Reynolds number is defined as:

$$Re = \frac{\rho VD}{\mu}$$

The Nusselt number is expressed as:

$$Nu = \frac{hD}{k}$$

The heat transfer rate (Q) was calculated using the measured mass flow rate and the temperature difference between the inlet and outlet of the fluid. The Reynolds number (Re) was evaluated to characterize the flow regime and assess the effect of flow velocity on heat transfer performance. The Nusselt number (Nu) was used as a dimensionless parameter to quantify the convective heat transfer enhancement, where the convective heat transfer coefficient (h) represents the intensity of heat transfer between the fluid and the tube wall, and the characteristic diameter (D) corresponds to the tube diameter

RESULTS AND DISCUSSIONS

Looking at the results overall, the corrugated tube performed better than the plain tube in every test condition, which is consistent with expectations from the literature. The corrugated surface repeatedly broke up the developing boundary layer and initiated secondary vortices in the near-wall region, keeping the convective heat transfer coefficient elevated relative to the smooth tube throughout the tested flow range. Experimentally measured temperatures and CFD predictions agreed reasonably well, with the CFD slightly over-predicting heat transfer at higher flow rates — probably a consequence of the k-ε model's known tendency to over-predict turbulence intensity in curved passages. Across the Reynolds number range tested, the corrugated configuration gave approximately 7–13% more heat transfer rate, a 6–10% larger temperature difference between inlet and outlet, and an 8–13% higher Nusselt number than the plain tube. Some additional friction loss came with the corrugations, but the thermal gain was clearly larger than the hydraulic penalty at all tested flow rates. These findings confirm what earlier studies have shown: corrugation is a simple and effective passive enhancement for this type of exchanger. The second part of the results — the polymer composite parametric study — builds on this foundation. By varying the wall conductivity from 0.2 to 20 W/m·K in the validated model, the analysis explores whether corrugation-generated turbulence can absorb the thermal penalty that comes with a lower-conductivity polymer wall.

As shown in Figure 5, it is observed that the heat transfer rate increases with an increase in flow rate for both the CFD-based corrugated tube analysis and the Bell–Delaware method. The Bell–Delaware method was used as a standard analytical method for shell-side calculations, included primarily as a validation reference rather than for design purposes. Both curves trend upward with flow rate, as the higher velocities raise the Reynolds number, suppress boundary layer growth, and increase the convective coefficient. The CFD values come out above the Bell–Delaware predictions throughout this is expected, since the analytical method does not account for the swirl and secondary structures that corrugation generates. From a polymer material standpoint, this corrugation-driven improvement on the fluid side is actually the more important number. When the tube wall is a low-conductivity polymer, the fluid-side convective resistance carries more of the overall thermal resistance burden, and anything that reduces it — corrugation being the main lever here — has a proportionally larger effect than it would in a metallic tube. At higher flow rates both the CFD and Bell–Delaware curves start to flatten, reflecting the shorter time the fluid spends inside the unit as velocity increases. The heat transfer rate is calculated from $Q = \dot{m}c_p(T_{in} - T_{out})$.

Figure 6 compares the three tube configurations side by side and shows the same upward trend for all of them as flow rate increases. The reasoning is straightforward: more flow means higher fluid velocity, a higher Reynolds number, and a thinner thermal boundary layer, each of which pushes the heat transfer rate up. Among the three, the finned tube delivers the highest heat transfer rate at every flow rate tested, which is not surprising given its combination of enlarged effective surface area and aggressive flow disturbance. The corrugated tube comes second, with the plain tube trailing behind. The corrugated tube's advantage over the plain tube — roughly 7–13% in heat transfer rate — comes primarily from the secondary flows and swirl that the corrugation profile induces, rather than any increase in total surface area.

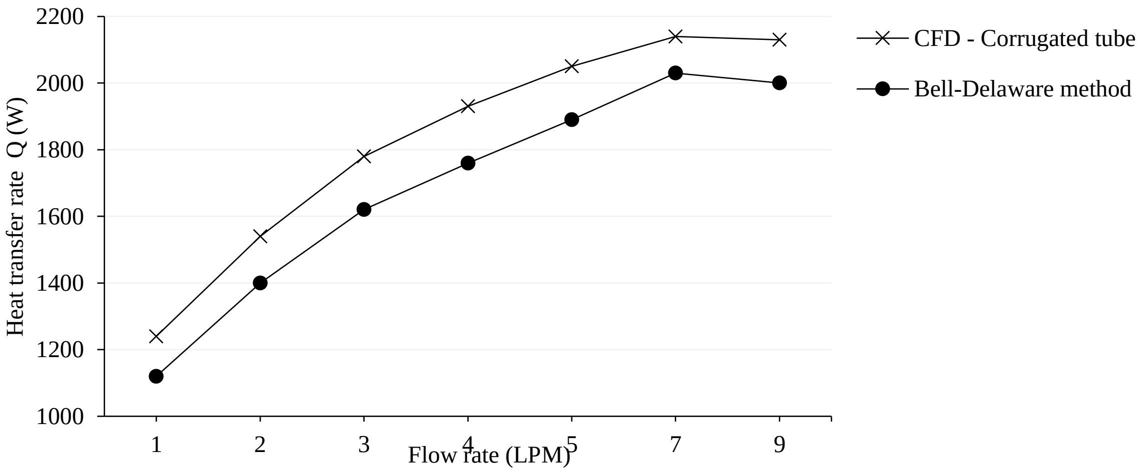

Figure 5. Comparison of heat transfer rate with respect to flow rate obtained from CFD analysis and Bell–Delaware method.

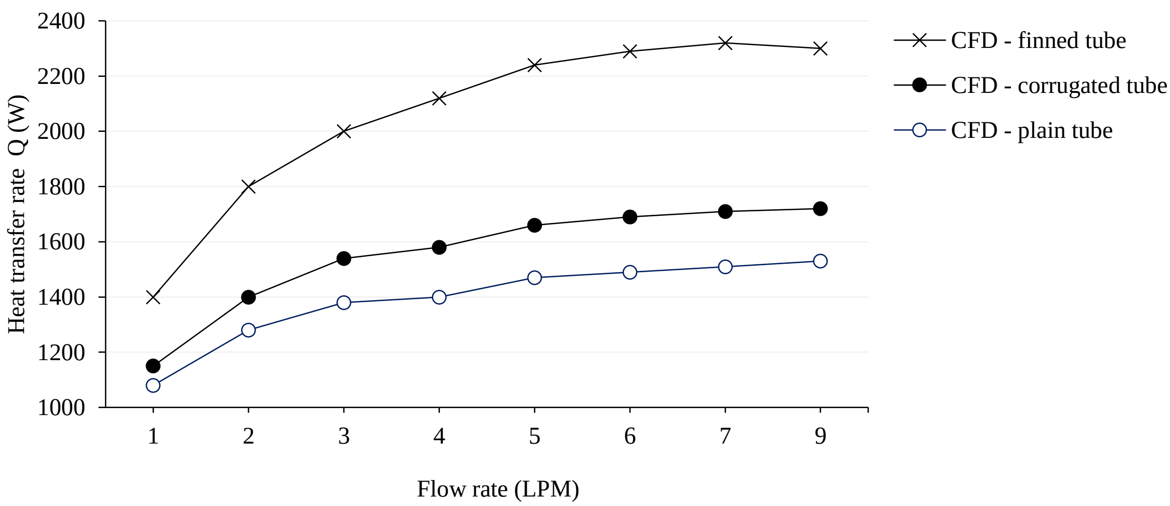

Figure 6. Variation of heat transfer rate with respect to flow rate for plain, corrugated, and finned tube configurations obtained from CFD analysis.

The plain tube, by contrast, allows a stable thermal boundary layer to establish and persist along most of its length, which is the limiting factor for its heat transfer. One practical implication of Figure 4 is that the corrugated tube closes a significant portion of the performance gap with the finned tube while likely being simpler to manufacture, making it a useful intermediate option for applications where the full complexity of a finned geometry is not warranted.

The temperature difference data in Figure 7 follow the trend that would be expected: ΔT falls as flow rate goes up in all three configurations. Higher flow rates push more mass through the exchanger per unit time, which reduces the residence time of any given fluid parcel and gives it less opportunity to exchange heat before exiting. At low flow rates, where the fluid spends longer inside the unit, the finned tube achieves the largest ΔT, the corrugated tube comes next, and the plain tube brings up the rear. This ordering is consistent throughout the tested range and matches the Nusselt number hierarchy. The corrugated tube's advantage over the plain tube — roughly 6–10% higher ΔT across the tested range — reflects the improved mixing and boundary layer disruption that the corrugated surface provides. One point worth noting is that higher ΔT, taken in isolation, does not necessarily mean better exchanger performance — it depends on what flow rate and duty the exchanger is sized for. The data in Figure 7 are most useful when considered alongside the heat transfer rate data in Figure 6. The observed trend is consistent with the relation Delta T is inversely proportional to m c□., which indicates that ΔT decreases as mass flow rate increases.

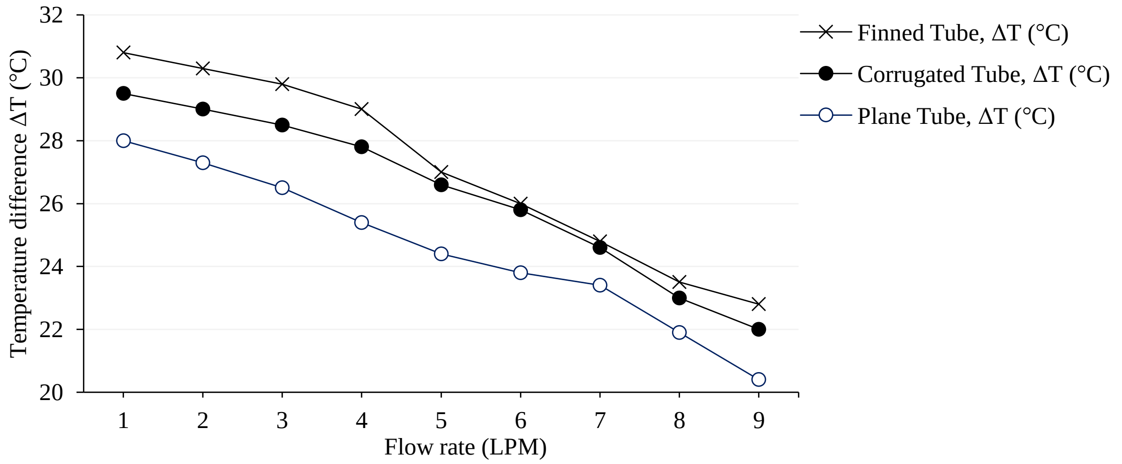

Figure 7. Variation of temperature difference (ΔT) with respect to flow rate for plain, corrugated, and finned tube configurations.

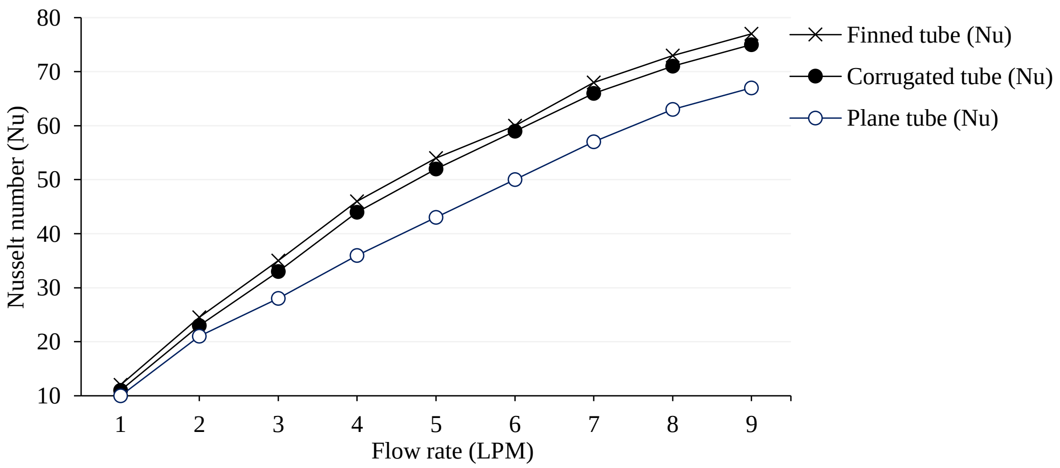

Figure 8. Variation of Nusselt number with respect to flow rate for plain, corrugated, and finned tube configurations.

The Nusselt number variation with flow rate is shown in Figure 8, where the expected rising trend with Reynolds number is evident for all three configurations. Higher flow velocity means a higher Reynolds number, stronger turbulence, and a thinner thermal boundary layer — all of which translate into a higher convective coefficient and therefore a higher Nu. The plain tube sits at the bottom throughout the tested range, reflecting the relatively stable boundary layer that forms in the absence of any surface enhancement. The corrugated tube achieves appreciably higher Nu values, which can be traced to the periodic flow separation, swirl generation, and repeated boundary layer re-initiation caused by the corrugation profile. These are not large-scale mixing effects — they are near-wall phenomena that directly reduce the thermal resistance at the surface.

The finned tube tops the Nusselt number chart at all flow rates, as expected from its combination of larger surface area and stronger flow disturbance. The corrugated tube comes in at 8–13% above the plain tube, which sits reasonably well with the Dittus–Boelter type correlation given the Reynolds number differences involved. Now, the important thing about Nusselt number for the polymer material question is that it is primarily a fluid-side quantity — it reflects the convective resistance at the wall surface and is only weakly dependent on what the wall is made of, provided the surface geometry stays the same. This means the corrugation-driven Nu enhancement that was measured with the metallic tubes applies to polymer composite tubes of the same profile as well. The CFD parametric runs with varied wall conductivity confirmed this: the Nusselt numbers were essentially unchanged across the conductivity range tested. What did change was the overall heat transfer rate, because the wall conduction resistance term in the overall thermal resistance adds more as conductivity drops. When the polymer composite wall conductivity exceeded about 4–5 W/m·K, the overall heat transfer rate stayed within roughly 10% of the stainless steel value. Drop below about 1 W/m·K — which is territory occupied by unfilled or lightly filled polymers — and the wall resistance starts to dominate the overall budget, with a more noticeable performance penalty. The practical message is fairly direct: a polymer composite tube for this application should be formulated to hit at least 4–5 W/m·K of effective conductivity. That is not an aggressive target — it is achievable with moderate loadings of graphite nanoplatelets or boron nitride.

CONCLUSIONS

This study examined how corrugating the tube surface affects the thermal performance of a U-tube shell-and-tube heat exchanger, and then used the same validated numerical model to explore what happens when the conventional stainless steel wall is replaced by a polymer composite with adjustable effective thermal conductivity. Experiments were conducted to validate the CFD predictions before extending the analysis to material properties that go beyond what was physically tested, and the agreement between measurements and simulations was satisfactory enough to justify that extension.

The corrugated configuration gave 7–13% more heat transfer rate, 8–13% higher Nusselt number, and 6–10% higher ΔT than the plain tube across the tested flow range. These gains come from the boundary layer disruption and near-wall mixing that corrugation induces, and they persist across all flow rates tested. Finned tubes did better in absolute terms because of their larger surface area, but corrugated tubes are simpler to manufacture and still provide a substantial step up over plain tubes. For the polymer material parametric study, the main finding is that effective wall conductivities above roughly 4–5 W/m·K keep the overall heat transfer rate within about 10% of the stainless steel baseline. This threshold is not out of reach — graphite nanoplatelet-filled or boron nitride-filled epoxy composites can hit these values at moderate filler loadings under standard processing conditions. The implication is that the performance gap between a corrugated polymer composite tube and a corrugated metallic tube can be made small enough to be acceptable in applications where the non-thermal advantages of polymer materials — corrosion resistance, lower weight — are valued.

Corrugation does add some friction — that is simply a consequence of introducing surface roughness — but the thermal gain is clearly larger than the hydraulic penalty across the operating range considered, which means corrugation is a worthwhile design choice here. Combining this with polymer composite tube materials, the picture that emerges is of a heat exchanger that might give up a few percent of peak heat transfer compared to its metallic counterpart, but in return gains significant durability in corrosive service environments and a lighter tube bundle. Whether that trade is worth making depends on the application, but the data suggest there is a meaningful subset of industrial cases where it would be. A number of questions were not addressed here and would be worth looking into. Long-term mechanical behaviour under thermal cycling is one — polymer composites can exhibit fatigue and creep that metals would not. Whether the filler orientation that develops during tube fabrication matches the assumptions behind the effective conductivity estimate is another. And there is probably scope to ask whether the corrugation profile currently used is the best choice for a lower-conductivity wall, or whether a different profile shape would give a better heat transfer-to-pressure drop ratio for polymer tubes specifically. The present results provide a useful reference point for any of those follow-on studies.

REFERENCES

1. Amin, N., et al. (2019). Multi-objective energy–economic optimization of shell-and-tube heat exchanger. Energy Conversion and Management, 180, 1–12.
2. Damdhar, A., Gunturkar, S., Dhumal, S., Jagtap, K., Pathak, A., Malkunjikar, S., & Kothmire, P. P. (2022). CFD analysis of exhaust gas flow through muffler. Proceedings of the Conference on Fluid Mechanics and Fluid Power, 599–613.
3. Deshmukh, S., Shinde, A., & Kothmire, P. P. (2023). Experimental study of heat transfer in composite vessels. Proceedings of the Conference on Fluid Mechanics and Fluid Power, 627–640.
4. Eiamsa-ard, S., & Promvonge, P. (2007). Enhancement of heat transfer in a tube with regularly spaced helical corrugations. Energy Conversion and Management, 48, 2278–2288.
5. Gadave, N. M., & Kothmire, P. P. (2019). Thermo-hydraulic performance evaluation of shell and tube heat exchanger with different tube geometries. International Journal of Engineering and Technology, 9, 2249–8958.
6. Gondane, S., & Jibhakate, B. (2016). CFD analysis of shell-and-tube heat exchanger using corrugated tubes. International Journal of Mechanical Engineering, 5, 45–52.
7. Gupta, R., & Pawar, S. (2017). Design and thermal performance analysis of shell-and-tube heat exchanger. International Journal of Thermal Sciences, 112, 90–99.
8. Kanate, V., Pardeshi, A., Charde, F., Kolase, K., Bhise, A., & Kothmire, P. P. (2022). Numerical investigation on performance of CPU heat sinks. Proceedings of the Conference on Fluid Mechanics and Fluid Power, 361–372.
9. Kishorkumar, P., et al. (2020). Experimental and numerical investigation of corrugated tubes in heat exchangers. Applied Thermal Engineering, 165, 114–122.
10. Kumavat, A., & Kothmire, P. P. (2023). CFD and experimental analysis for optimal cooling system design in theatres. Proceedings of the Conference on Fluid Mechanics and Fluid Power, 483–496.
11. Li, H., et al. (2019). Influence of segmental baffle design on shell-side heat transfer performance. Applied Thermal Engineering, 148, 842–853.
12. Londhe, S., Auti, V., Kothmire, P. P., et al. (2023). Impact of economiser tube geometry on water heating. Proceedings of the Conference on Fluid Mechanics and Fluid Power, 275–287.
13. Maheshwari, P., & Trivedi, J. (2019). Experimental investigation of U-tube heat exchanger with corrugated tubes. Heat and Mass Transfer, 55, 1789–1798.
14. Nagarhalli, P., Mayekar, A., Pakhare, R., Pachkudave, T., Bhalerao, Y., & Kothmire, P. P. (2023). Natural and forced convective heat transfer from finned spheres. Proceedings of the Conference on Fluid Mechanics and Fluid Power, 365–379.
15. Narad, V., Malu, P., Giri, P., Borole, S., Naikare, A., & Kothmire, P. P. (2022). Numerical investigation to study the effective position of air conditioner in an office room. Proceedings of the Conference on Fluid Mechanics and Fluid Power, 209–220.
16. Nawale, P. K., Mule, A., Powar, S., & Kothmire, P. P. (2021). Enhancement technique of heat transfer using inserted twisted tape. Journal of Thermal Engineering, 9, 93–99.
17. Pawar, A., Halikhede, S., Umbarkar, A., Kedar, A., Waghmode, P., & Kothmire, P. P. (2022). CFD

analysis of different designs of greenhouse. Proceedings of the Conference on Fluid Mechanics and Fluid Power, 277–288.

18. Powar, S., Chitrakar, N., Chacharkar, L., Adarsh, P., Karhale, S., Patil, R., & Kothmire, P. P. (2022). Effect of surface roughness on boundary layer thickness. Proceedings of the Conference on Fluid Mechanics and Fluid Power, 371–380.
19. Serrao, A., et al. (2018). Comparative study of heat transfer in plain and corrugated pipes. International Journal of Heat and Mass Transfer, 120, 856–864.
20. Shindge, M., Dhamnikar, P., Tamboli, S., Fulzele, R., Gatlewar, O., Funde, A., & Kothmire, P. P. (2022). CFD analysis of catalytic converter to optimize back pressure and velocity. Proceedings of the Conference on Fluid Mechanics and Fluid Power, 289–303.
21. Singh, V., & Jha, R. (2017). Numerical investigation of corrugated heat exchanger configurations. Applied Thermal Engineering, 115, 115–124.
22. Tajane, Y., Lohar, P., Ghangar, G., Eshi, M., & Kothmire, P. P. (2023). Experimental and CFD investigation of radiative heat transfer for room cooling. Proceedings of the Conference on Fluid Mechanics and Fluid Power, 337–350.
23. Vicente, P. G., et al. (2004). Experimental investigation of heat transfer in spirally corrugated tubes. International Journal of Heat and Mass Transfer, 47, 671–681.
24. Yadav, P., & Kothmire, P. P. (2021). CFD analysis of exhaust pipe of a diesel engine. AIP Conference Proceedings, 2417, 060002.
25. Chung, D. D. L. (2022). Polymer–matrix composites for thermal management: a review. Journal of Materials Science, 57, 8602–8640. https://doi.org/10.1007/s10853-022-07196-3
26. Huang, C., Qian, X., & Yang, R. (2023). Thermal conductivity of polymers and polymer nanocomposites. Materials Science and Engineering: R: Reports, 132, 100570. https://doi.org/10.1016/j.mser.2018.06.002
27. Pandey, R., Jeong, H. M., & Kim, C. H. (2021). Heat transfer performance of polymer heat exchanger with enhanced surface geometries: an experimental investigation. International Journal of Heat and Mass Transfer, 168, 120891. https://doi.org/10.1016/j.ijheatmasstransfer.2020.120891
28. Wu, H., Drzal, L. T., & Liang, X. (2020). Graphene nanoplatelet paper as a light-weight composite with excellent electrical and thermal conductivity and good gas barrier properties. Carbon, 158, 418–427. https://doi.org/10.1016/j.carbon.2019.11.006
29. Ramasubbu R, Kayambu A, Palanisamy S, Ayrilmis N. Mechanical properties of epoxy composites reinforced with Areca catechu fibers containing silicon carbide. BioResources. 2024;19(2):2353–2370.
30. Palanisamy S, Mayandi K, Dharmalingam S, Rajini N, Santulli C, Mohammad F, Al-Lohedan HA. Tensile properties and fracture morphology of Acacia caesia bark fibers treated with different alkali concentrations. Journal of Natural Fibers. 2022;19(15):11258–11269.
31. Mylsamy B, Aruchamy K, Shanmugam SKM, Palanisamy S, Ayrilmis N. Improving performance of composites: Natural and synthetic fibre hybridisation techniques in composite materials – A review. Materials Chemistry and Physics. 2025;334:130439.
32. Manickaraj K, Karthik A, Palanisamy S, Jayamani M, Ali SK, Lakshmi Sankar S, Al-Farraj SA. Improving mechanical performance of hybrid polymer composites: Incorporating banana stem leaf and jute fibers with tamarind shell powder. BioResources. 2025;20(1):1998–2025.
33. Karlekar, O., Galande P., Pol O., Barve, S., & Kothmire, P. Thermo-Hydraulic Enhancement of Annular Finned Shell-and-Tube Heat Exchangers Using Epoxy-Based Polymer Composites: A Material–Geometry Coupled CFD Investigation, Journal of Polymer & Composites. 2026;14(Special Issue 02):669–684.
34. Karkal P, Barve S, Kothmire PP. Experimental and CFD investigation of an epoxy-based thermally conductive polymer composite U-tube shell-and-tube heat exchanger. Journal of Polymer & Composites. 2026;14(Special Issue 02):685–700.
35. Patil R, Kamble S, Kokare P, Goudar M, Kothmire PP. Investigation to enhance performance of finned U-tube shell-and-tube heat exchangers using epoxy based polymer composite. Journal of Polymer & Composites. 2026;14(Special Issue 02):618–633.

36. Patel A, Gujar S, Bhalerao Y, Kothmire PP. Influence of epoxy-based thermally conductive polymer composites on the thermo-hydraulic performance of finned helical coil heat exchangers. Journal of Polymer & Composites. 2026;14(Special Issue 02):586–602.
37. Dabhade T, Gawari T, Nawale P, Shah B, Jain S, Kothmire PP. Corrugated tube shell-and-tube heat exchanger using epoxy-based polymer composite coatings for lightweight and efficient thermal systems. Journal of Polymer & Composites. 2026;14(Special Issue 02):603–617.
38. Dhanawade N, Joshi S, Wankhade P, Bhalerao V, Kothmire PP. Thermal dissipation performance of metal–polymer composite heat exchanger for enhanced thermal management in compact geysers. Journal of Polymer & Composites. 2026;14(Special Issue 02):618–651.
39. Kapure S, Rathod P, Patil A, Rai H, Kothmire PP. Multiphysics optimization of polymer–metal hybrid electrode geometry in electrostatic precipitators. Journal of Polymer & Composites. 2026;14(Special Issue 02):701–716.
40. Mankar B, Gopale Y, Balghare S, Jadhav P, Kothmire PP. Thermo-electrical performance enhancement of a lightweight polymer–metal hybrid electrostatic precipitator. Journal of Polymer & Composites. 2026;14(Special Issue 02):652–668.
41. Dixit S, Londhe K, Patil A, Kanase S, Goudar M, Kothmire PP. Characterization and performance of a multiphase lignocellulosic–polymeric composite growth media in an IoT-automated NFT hydroponic system. Journal of Polymer & Composites. 2026;14(Special Issue 02):542–555.

